BMP-Induced osteogenesis on the surface of hydroxyapatite with geometrically feasible and nonfeasible structures: Topology of osteogenesis

Y. Kuboki,[1] H. Takita,[1] D. Kobayashi,[1] E. Tsuruga,[1] M. Inoue,[2] M. Murata,[2] N. Nagai,[2] Y. Dohi,[3] H. Ohgushi[4]

[1]*Department of Biochemistry, School of Dentistry, Hokkaido University, Kita 13, Nishi 7, Kita-ku, Sapporo, Japan 060*
[2]*Department of Oral Pathology, School of Dentistry, Okayama University, Okayama, Japan 700*
[3]*Department of Public Health, Nara Medical University, Nara, Japan 634*
[4]*Department of Orthopedic Surgery, Nara Medical University, Nara, Japan 634*

Received 4 December 1996; accepted 24 January 1997

Abstract: Bone morphogenetic protein (BMP) is known to require a suitable carrier to induce ectopic bone formation *in vivo.* Hydroxyapatite ceramics have been reported to be effective in some forms but ineffective in others as a carrier of BMP-induced bone formation. In this study we compare three geometrically different forms of hydroxyapatite to examine their functions as carriers of BMP-induced bone formation. A fraction containing all the active BMPs (BMP cocktail) was partially purified from a 4*M* guanidine extract from bovine bone by a three-step chromatographic procedure. The BMP cocktail was combined with each of three forms of hydroxyapatite—solid particles (SPHAP), porous particles (PPHAP), and coral-replicated porous tablets (coral-HAP)—and implanted subcutaneously into rats. Both the PPHAP and coral-HAP systems induced osteogenesis 2 weeks after implantation, as evidenced by morphological and biochemical observations. Details of the osteogenetic process were followed by double-fluorescence labeling in the coral-HAP system to confirm bone formation on the surface of hydroxyapatite. However, there was no evidence of osteogenesis or chondrogenesis in the SPHAP system. The results indicate that the geometry of the interconnected porous structure in PPHAP and coral-HAP create spaces for vasculature that lead to osteogenesis while the smooth structure and close contact of particles in SPHAP inhibit vascular formation and proliferation of mesenchymal cells, preventing bone and cartilage formation. It was concluded that the geometrical structure in hydroxyapatite ceramics that induces vasculature is crucial as a carrier for BMP-induced bone formation. © 1998 John Wiley & Sons, Inc. *J Biomed Mater Res,* **39,** 190–199, 1998.

Key words: BMP; geometry; carriers; hydroxyapatite

INTRODUCTION

To elucidate the biochemical mechanism of bone formation, it is proposed that, at least stradically, four factors must be taken into consideration.[1–4] They are: (1) cells directly involved in bone formation, (2) matrices produced by the cells, (3) body fluid, including mineral ions, and (4) regulators of general cellular activities as well as of the calcification process. These four factors should be analyzed individually, then the interactions between them elucidated; finally, they should be integrated into the whole picture of bone formation. The principle can be applied not only to understand the mechanism of bone formation but also to reconstruct bone tissue locally *in vivo* and *in vitro.*

To verify the above proposition, we chose ectopic osteo- and chondrogenesis induced by BMP[5–7] as our experimental system because cells and body fluid already are available in this system. The only items we had to add to induce cartilage and bone formation were the matrix and regulators. BMP-induced chondro- and osteogenesis in ectopic tissues, such as skin and muscles, originally were discovered by Urist et al. in 1965.[8] The proteins called BMP were found to be members of the TGF-β supergene family by cloning and sequencing their DNA.[9] Also, it was found that BMPs consist of multiple members of the BMP family, BMP-2 to BMP-13.[10]

One of the most interesting aspects of BMP-induced chondro- and osteogenesis is that a purified or recombinant BMP needs a certain carrier to induce the *in vivo* cartilage or bone formation.[1,5–7] At first the phe-

Correspondence to: Y. Kuboki, e-mail address: kuboki@den.hokudai.ac.jp

 CCC 0021-9304/98/020190-10

nomenon was explained by the rapid diffusion from the point of administration when it was applied to muscles or skin without a carrier. Thus the BMP carrier was considered to be a typical drug delivery system. But soon it was shown that the BMP carrier is not merely a drug delivery system but also an important cell supporter for differentiation since bone formation occurs only on the surface of the carrier.[11,12]

Consistent with the above concept, it was found that BMP-induced chondro- and osteogenesis are highly dependent upon the carrier used in the experimental system.[11] The most widely used carrier of BMP is insoluble bone matrix, which is the decalcified and 4*M* guanidine-extracted residues of bone powder or tips.[12] Insofar as insoluble bone matrix has been used as a carrier, BMP has been considered to be a cytokine that induces a process similar to endochondral ossification; that is, osteogenesis occurs only after chondrogenesis. However, by using another carrier, fibrous collagen membrane, Sasano et al. showed for the first time that BMP can induce direct bone formation independent of cartilage formation.[6] Furthermore, our laboratory (Kuboki et al.) showed that BMP alone induces osteogenesis without any chondrogenesis when porous particles of hydroxyapatite are used as one carrier whereas only chondrogenesis occurs within the carrier when a fibrous glass membrane is used as a carrier.[11] We concluded that vasculature is the crucial factor that determines osteogenesis or chondrogenesis.

More recently, Saito et al.[13] and Sasaki et al.[14] showed that BMP combined with a fibrous collagen membrane induces not only bone, but also regenerates cementum and the periodontal ligament when it is implanted into periodontal defects in the cat, canine,[13] and monkey molar,[14] respectively. These observations led us to the working hypothesis that BMP-induced cell differentiation is highly dependent on the cell substratum, that is, the matrix, and on microenvironmental conditions, and that this cell substratum and the microenvironment are provided by BMP carriers.

The essential characteristics of BMP carriers are classified into three categories: chemical, physical, and geometric. The first two categories are mainly concerned with biocompatibility, cell attachment, and affinity for biomolecules. These categories are well documented. However, the significance of the geometry of BMP carriers has not been studied and understood except in a very limited sense. Also, there have been some discrepancies concerning the efficacy of hydroxyapatite as a carrier for BMP. Ripamonti and Reddi reported that disk-formed porous hydroxyapatite was effective, but a granular form of the same material was not. These results are inconsistent with our findings.[11]

Thus, in this paper we demonstrate that both porous particles of hydroxyapatite (PPHAP) and coral-replicated hydroxyapatite (coral-HAP) function as effective carriers of BMP for osteogenesis while solid particles of hydroxyapatite (SP-HAP) do not function as a BMP carrier under the same experimental conditions. The results clearly indicate that BMP-induced bone formation is highly dependent upon the geometry of the carrier and that BMP when it is combined with hydroxyapatite that has a structure geometrically suitable for vascularization is able directly to induce immature cells into becoming osteogenetic cells that form a bone-like structure.

MATERIALS AND METHODS

Preparation of BMP cocktails

Freshly obtained bovine metatarsal bones were powdered in a stainless steel mortar and pestle while being cooled under liquid nitrogen and sieved to obtain particles smaller than 60 mesh.[15,16] Preparation of partially purified BMP was done according to the method reported.[17] The bone powder (1 kg per extraction) was washed with 1.0*M* NaCl, 50 m*M* Tris-HCl, pH 7.4 (including protease inhibitors: 50 m*M* aminocaproic acid, 5 m*M* benzamidinehydrochloride, 1 m*M* benzylsulfonylfluoride), and defatted with $CHCl_3/CH_3OH$ (1:1). The processed bone powder then was demineralized in diluted HCl, keeping the pH constant at 2.0 by adding 12*N* HCl. The demineralized bone matrix was extracted with 4*M* of guanidine hydrochloride in 50 m*M* Tris-HCl, pH 7.4, containing the protease inhibitors described above. The extracts were centrifuged (15,000 rpm, 30 min, 4°C) and the supernatants were filtered through a Nucleopore membrane (3 mm, Nucleopore, Co., Pleasanton, CA). A detailed description of the procedure used for purification of the active fraction of the guanidine extract by an eight-step chromatographic procedure has been published.[17] The final active preparation was shown by internal sequence analysis (residues 410–424) of trypsin digestion to contain at least a significant amount of BMP-3. In the present study, a partially purified BMP fraction treated by the three-step chromatographic procedure described below was used.

A column (8.3 × 12 cm, 500 mL) packed with hydroxyapatite (FK-1, Apatite International, Co., Tokyo) was equilibrated with 1 m*M* potassium phosphate buffer containing 6*M* of urea (pH 6.8), and the applied sample was eluted in a stepwise manner with 0.1 and 0.4*M* of phosphate ions in a potassium phosphate buffer containing 6*M* of urea (pH 6.8). The activity was recovered in a 0.4*M* phosphate fraction, which was concentrated and replaced with the buffer used in the chromatography. On a Heparin-Sepharose CL-6B column (Pharmacia LKB: 3 × 30 cm, 190 mL) equilibrated in 0.1*M* NaCl, 50 m*M* Tris-HCl, and 6*M* Urea, pH 7.0, the applied sample was eluted with 0.1, 0.15, and 0.5*M* NaCl in a stepwise manner. The activity was recognized in a 0.5*M* NaCl elution fraction, which was concentrated and replaced with the next solvent. Sephacryl S-300 HR (Pharmacia Uppsala: 2.2 × 141 cm, 500 mL) was equilibrated with 4*M* guanidine-HCl/50 m*M* Tris-HCl, pH 7.4, and eluted with

the same buffer. The BMP-containing fractions were pooled and designated S-300. The S-300 BMP preparation was pooled from at least five extractions in order to keep its quality constant.

One unit of BMP activity in this study was defined as follows: the amount of S-300 or any other BMP preparation that induced a calcium content as high as 20% of the dry implant when it was implanted with 20 mg of IBM and harvested after 2 weeks.

Preparation of BMP/carrier composites

Coral-replicated hydroxyapatite

This carrier, consisting of blocks of a porous hydroxyapatite replica in disk form (5 mm in diameter and 2 mm in height), was a gift from Interpore International, Irvine, CA. Briefly, the exoskeletal microstructures of calcium carbonate of corals (genus Porites) were converted into hydroxyapatite by hydrothermal chemical exchange.[18] The average pore diameter and porosity of the implant were 230 μm and 66%, respectively.

Porous particles of hydroxyapatite (PP-HAP)

Porous particles of hydroxyapatite were developed jointly by the Department of Biochemistry, School of Dentistry, Hokkaido University, and Japan Steel Works, Ltd. (Muroran, Japan). The product consisted of a block of hydroxyapatite with a porosity of 70%, a pore size of 150 μm, and block sizes of 3 × 3 × 1.5 mm. It was sintered at 1200°C. The procedure for preparation has been reported in detail.[19] Briefly, the hydroxyapatite was synthesized by the method reported previously.[20] The HAP powder was mixed with specific amounts of spherical acrylic beads (30:70 in volume), sieved to 100–200 μm in diameter, cold-isostatic pressed under a pressure of 3,000 kg/cm^2, and broken into granules. After the acrylic resin was removed by heating it slowly to 600°C in a nitrogen atmosphere, the HAP was sintered at 1200°C for 1 h. Granules were sieved to obtain a fraction in which the particle size ranged from 0.3 to 0.5 mm. One of the characteristics of the product is that its pores are connected, so that spaces open continuously in each particle.[11]

Solid particles of hydroxyapatite (SP-HAP)

Except for its not being mix with acrylic beads, hydroxyapatite powder was synthesized by the same method described above and was cold-isostatic pressed under the same conditions as above. It then was broken into granules. These granules were heated as described above and sieved to obtain a particle size ranging from 0.3–0.5 mm.

Combination of BMP and carriers

One half unit of the S-300 BMP (0.30 mg) in phosphate-buffered saline was absorbed into each hydroxyapatite and stored at −20°C until use.

Implantation of carrier/BMP complex

Using a 1 mL tuberculin syringe, the top portion of which was cut open,[16] the carrier/BMP complex and control, which contained collagen instead of BMP, were implanted subcutaneously in the backs of rats (Wistar strain, male, 4 weeks old) for ectopic osteogenesis.

Biochemical analysis

The implants were removed at week 1, 2, 3, or 4. Alkaline phosphatase (ALP) activity and the calcium and osteocalcin contents in the implants were determined to evaluate the phenotype expression. ALP activity was measured by the phenyl-phosphate method (Kind–King method);[21] calcium content was measured by the orthocresolphthalein-complexone (OCPC) method;[22] and protein content was measured by the bicinchoninic acid method.[23]

Osteocalcin in the implant was extracted by shaking in 5 mL of 20% formic acid for one week at 4°C. An aliquot of the formic acid extract then was applied to a column of Sephadex G-25 and eluted with 10% formic acid. Protein fractions were collected, lyophilized and used for radioimmunoassay of osteocalcin, as previously described.[24]

Fluorescent labeling of newly-formed bone

The rats were intramuscularly given one dose each of tetracycline (100 mg/kg) 13 days after implantation and calcein (7.5 mg/kg) 19 days after implantation. Animals were killed 21 days after implantation.

Undecalcified histological sections and SEM observation

Implants were fixed in 70% ethanol and stained with Villanueva bone stain. They then were dehydrated in a graded series of ethanol and acetone. After embedding in methyl methacrylate, the implant surface was cut out into sections of 7 μm using a Jung Model K microscope. These specimens were observed under light microscopy or fluoromicroscopy. For scanning electron microscopy and electron probe microanalysis (SEM-EPMA), the surface of the implant embedded in methyl methacrylate was coated with a thin layer of carbon, and the ceramic/bone interface was analyzed by using a scanning electron microanalyzer connected with a wavelength dispersive spectrometer.

RESULTS

Morphological observation

Coral-HAP/BMP composites

Figure 1(A) shows a cross-section of coral-HAP/BMP composite harvested at 1 week after implanta-

tion. Most areas within the pores and outside of the coral HAP (indicated by C) were filled with fibrous tissue. There was no bone formation, but a small amount of cartilage formation was found occasionally. At 2 weeks after implantation, coral-HAP/BMP exhibited early bone formation (indicated by the arrow) on the inner surface of the pores of the ceramic (indicated by C), as shown in Figure 1(B). Bone formation became extensive 3 weeks after implantation. As shown in Figure 1(C), bone formation could be seen inside of the pores and on the outer surface of the ceramic disk. Figure 1(D) shows a higher magnification of the area enclosed in the rectangle in Figure 1(C). Active bone formation (arrow) on the surface of the ceramic (C) could be clearly seen. Bone occupied a considerable part of the area within the pores.

Without BMP, as shown in Figure 1(E), the coral-HAP control, which contained collagen instead of BMP, did not induce any bone or cartilage formation at 3 weeks after implantation. Only fibrous tissue formation (indicated by F) with vascularization (arrow) could be seen in the pores of the ceramic (C).

Detailed changes in the bone-forming area were observed by double fluorescence labeling (Fig. 2) and SEM with an X-ray microanalyzer (Fig. 3). First, as seen in Figure two relatively sharp tetracycline-deposited bone layers were observed along the surface of coral-HAP (indicated by H in Fig. 2) at a certain distance from the surface. Next, outside of the tetracycline layer, relatively diffuse calcein-deposited layers that almost directly contacted the uncalcified tissue (indicated by U in Fig. 2) were observed. Since tetracycline and calcein were injected at 13 and 19 days after implantation, respectively, the tetracycline-deposited layer indicated that the bone had formed between days 13 to 19, and the calcein-deposited layer indicated that it had been formed thereafter by day 21. It was noted that both layers were irregular in thickness and intensity, but they generally surrounded the coral-HAP. Figures 3(A) and 3(B) show a back-scattered electron image and electron probe micro-analysis, respectively, of the interface between the coral-HAP/BMP and newly formed bone. A relatively darker layer of newly formed bone directly attached to the coral-HAP clearly was seen. The calcium and phosphorus contents in the newly formed bone (the darker part of the area indicated by B) almost were equivalent to the coral-HAP (the brighter part of the area indicated by H) and suddenly dropped at the sub-surface layer, which might express uncalcified osteoid.

PPHAP/BMP composite

In PPHAP/BMP composites, active bone formation was observed at 3 weeks after implantation. The efficacy of PPHAP as a BMP carrier already has been verified and reported.[11] Figure 4(A) shows bone formation in PPHAP; particles appeared to be connected to each other so that vasculature was able to invade continuously. The borders of the particles were difficult to discern. An enlarged picture of bone formation within the pores of PPHAP is shown in Figure 4(B). Most of the space within the pores [P in Fig. 4(B)] and between the particles [S in Fig. 4(B)] was occupied by bone, but it should be noted that in every pore there was a small space left for vasculature.

SPHAP/BMP

Figure 5 shows a cross-section of the SPHAP/BMP implant taken 3 weeks after implantation. SPHAP were surrounded by fibrous connective tissue, but there was no bone or cartilage formation at all throughout the experimental period (up to 3 weeks). Neither bone nor cartilage was observed even when 0.5 mg of S300 BMP was administered with SPHAP.

Biochemical observation

ALP activity and osteocalcin in coral-HAP/BMP

In Figure 6, time-dependent changes of alkaline phosphatase activity in the coral-HAP/BMP and coral-HAP alone are shown. In the implants of the coral-HAP alone there was no detectable activity of ALP. With the addition of BMP, the maximum activity of ALP in the implants already had been attained only 1 week after implantation. The activity decreased rapidly until 3 weeks.

In Figure 7, time-dependent changes of osteocalcin in the coral-HAP/BMP are shown. In the implant of coral-HAP alone there was no detectable osteocalcin. Osteocalcin contents in the coral-HAP rose rapidly at 2 weeks, then slightly increased at 3 weeks. For PPHAP/BMP, ALP activity and osteocalcin contents were highly reproducible compared with a study we reported previously,[11] which had been carried out under exactly the same conditions. Therefore, the results are not shown in this paper. Also, values of ALP activity and osteocalcin contents in PPHAP/BMP were almost equivalent with those of the coral-HAP/BMP throughout the experimental study.

Dry weight and ALP activity in SPHAP

In Figure 8, time-dependent changes of dry weight and alkaline phosphatase activity in SPHAP/BMP and SPHAP alone are shown. The dry weight of the

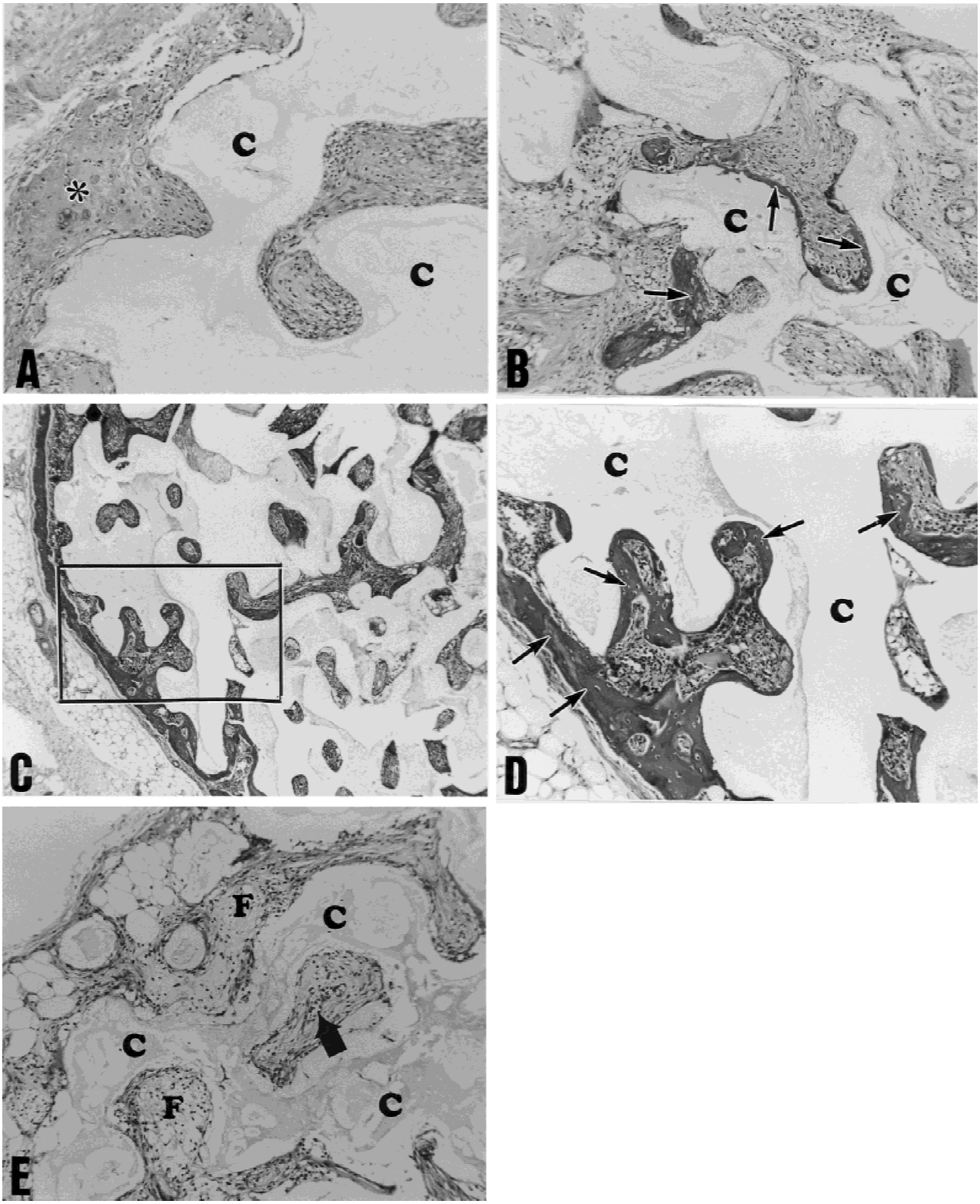

Figure 1. (A) Photomicrograph of the coralline-replicated hydroxyapatite combined with BMP (coral-HAP/BMP) harvested at 1 week after implantation. Most areas within the pores and outside of the coral HAP (indicated by C) were filled with fibrous tissue. There was no bone formation, but cartilage formation (indicated by asterisk) was found occasionally. Hematoxylin and eosin stain, original magnification, ×100. (B) Photomicrograph of the coral HAP/BMP harvested at 2 weeks after implantation. Early bone formation (indicated by arrow) can be seen on the inner surface of the pore of the ceramic (indicated by C). Hematoxylin and eosin stain, original magnification, ×100. (C) Photomicrograph of the coral HAP/BMP harvested at 3 weeks after implantation. Extensive bone formation is seen inside and outside of the pores. Hematoxylin and eosin stain, original magnification, ×40. (D) Magnified photomicrograph of the rectangular area in Figure 1(C). Bone formation (arrows) is clearly seen occupying most of the area within the pores. (E) Photomicrograph of coral HAP control, which contained collagen instead of BMP, harvested at 3 weeks after implantation. Only fibrous tissue formation (indicated by F) together with vascularization (arrow) can be seen in the pore area of the ceramic (indicated by C). No bone formation can be seen. Hematoxylin and eosin stain, original magnification, ×100.

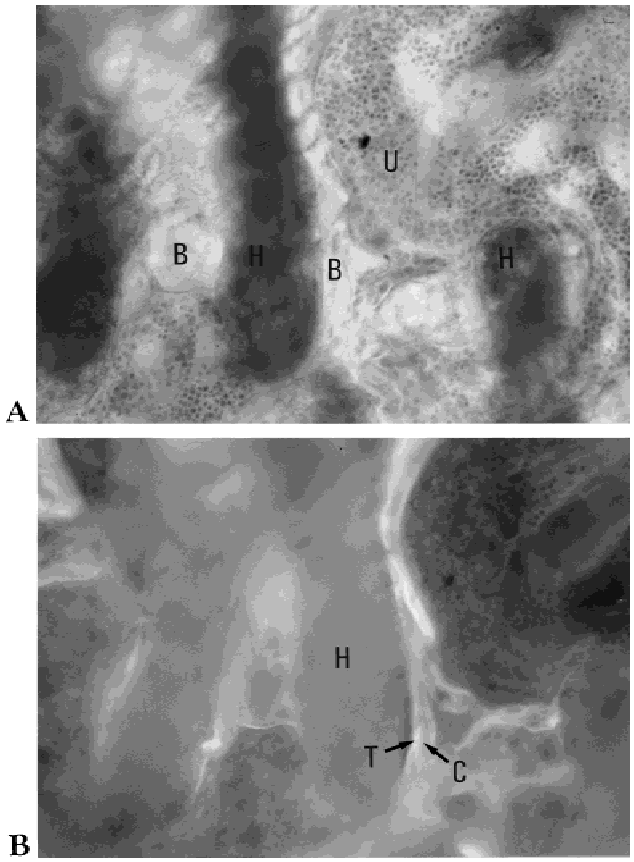

Figure 2. (A) Photomicrogram showing an undecalcified section of coral-HAP/BMP harvested at 4 weeks after implantation. B, newly formed bone; H, coral- HAP; U, uncalcified tissue. (B) The same section under fluoromicroscopy showing an undecalcified section of coral-HAP/BMP. Relatively sharp tetracycline-deposited bone layers (indicated by T, yellow) were observed along the surface of coral-HAP (indicated by H) with a certain distance between them. Outside of the tetracycline layer, relatively diffuse calcein-deposited layers (indicated by C, green) that almost directly contacted the uncalcified bone were observed. Tetracycline and calcein were injected at 13 and 19 days, respectively, and animals were killed at 28 days after implantation. Original magnification, ×100.

implant of SPHAP/BMP was higher than that of SPAHP alone, but there was no significant ALP activity either in the SPHAP or SPHAP/BMP. Figure 8(B) shows that ALP activities in SPHAP/BMP were almost at the level of experimental error.

DISCUSSION

Direct bone formation and vasculature

Coral-HAP/BMP and PPHAP/BMP composites definitely induced bone formation, as evidenced by histological observation, alkaline phosphatase activity, and increases of osteocalcin. However, SPHAP/BMP did not induce bone or cartilage at all. Considering that the synthetic procedures used to make hydroxyapatite for PPHAP and SPHAP were identical, the fact that bone induction was observed only in PPHAP reasonably can be ascribed to its porous geometry. Thus, our study clearly indicated that BMP-induced bone formation is highly dependent upon the geometry of the carrier. Also, PPHAP exclusively induced direct bone formation, without any detectable cartilage formation. This result was exactly the same as that we already have reported.[11] Thus, we propose that BMP, if it is combined with hydroxyapatite having a geometrically feasible structure, is able to induce immature cells directly into becoming osteogenic cells that cause membraneous ossification or harvarsian bone formation without cartilage formation. This ob-

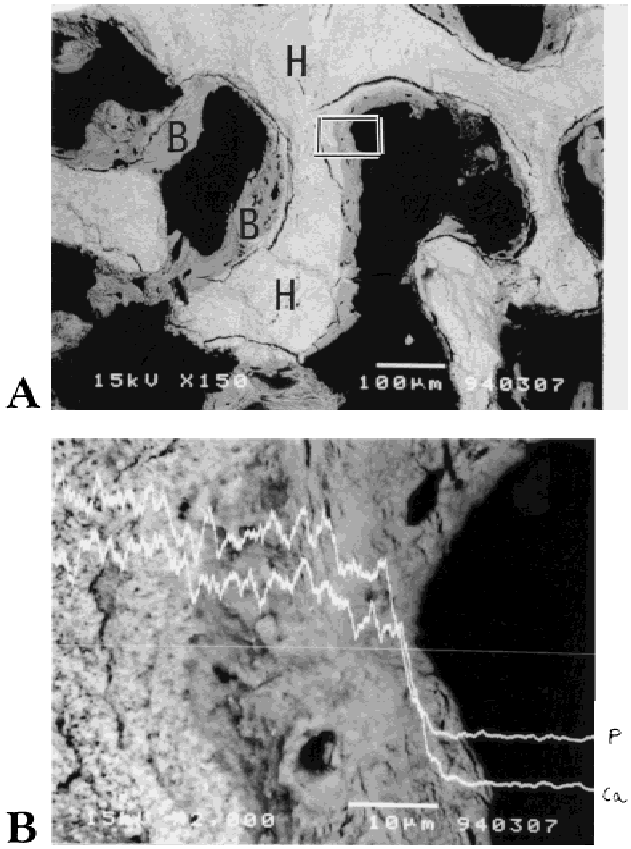

Figure 3. SEM and X-ray microanalysis of the coral-HAP/BMP at 3 weeks after implantation. Figures 3(A, B) show a back-scattered electron image and a SEM pattern, respectively, of the interface between the coral-HAP and the newly-formed bone. In Figure 3(A) it clearly can be seen that a relatively darker layer of newly formed bone is directly attached to the coral-HAP. The calcium and phosphate contents in the newly formed bone (the darker part of the area, indicated by B) were almost equivalent to the coral-HAP (the brighter part of the area, indicated by H) and suddenly dropped at the sub-surface layer, which might express uncalcified osteoid.

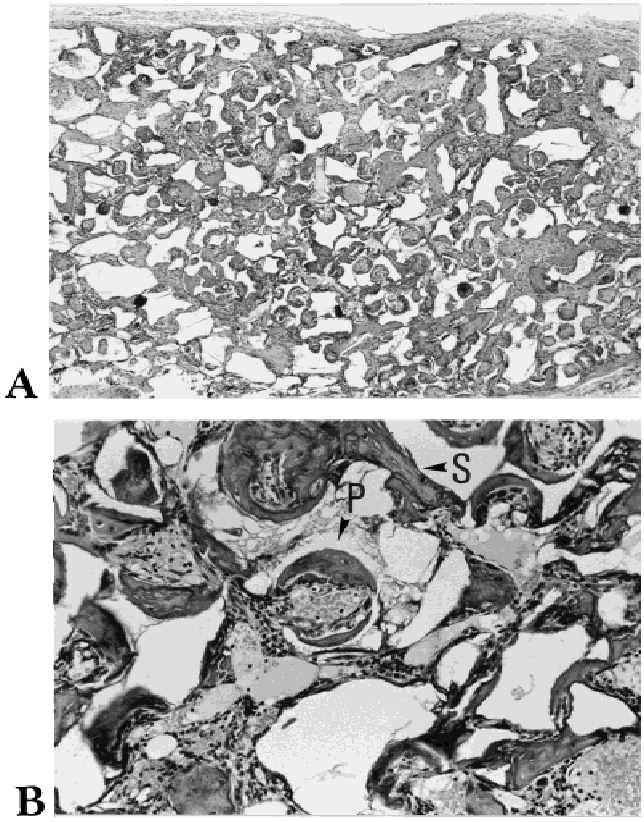

Figure 4. Photomicrographs of the porous particles of hydroxyapatite combined with BMP (PPHAP/BMP) harvested at 3 weeks after implantation. (A) In most of the pores and the spaces between the particles, bone was formed starting from the surface of PPHAP. (B) Magnified micrograph of the rectangular area in Figure 4(A). Bone formation occurred in the pores (indicated by P) and the spaces (indicated by S) between the particles. Bone formation in the pores always left blood vessels in the central portion. Note erythrocytes and lining osteoblasts in the central portion of the pores.

servation is quite different from the traditional view that BMP-induced bone formation is essentially endochondral ossification.[25–27] In contrast to the finding of bone formation in PPHAP/BMP, some areas of coral-HAP/BMP showed cartilage formation [Fig. 1(A)]. However, the areas were restricted and the incidence was very low. Perhaps this was due to the irregularity or a disturbance of interconnective pores of the coral structure during the manufacturing process. Thus the general cascade of the bone formation induced by BMP in the pore area of coral-HAP was assumed to be as follows: undifferentiated fibroblastic cells attached to the surface of the pores where osteoblastic differentiation occurred, resulting in the production and deposition of a calcifiable matrix that was firmly attached to the ceramic surface [Figs. 1(B) and 3]. Additionally, vasculature through the interconnected pores provided a favorable condition for direct bone formation without cartilage formation.

Geometry of cell substratum and carrier

In 1973, Reddi and Huggins pointed out that cell differentiation is highly dependent on the geometry of the cell substratum.[28] They reported that allogenic implants of demineralized ''tooth tube'' and conical whole tooth induced utterly different types of chondrogenesis and osteogenesis. They concluded that a hypoxic environment in the apex of the conical pulp chamber or middle portion of the tooth tube favors chondrogenesis. They also reported that a coarse powder (420–850 μm) of demineralized bone induces a much higher yield of bone than does a fine one (44–74 μm). Later, Sampath and Reddi reported different efficiencies for coarse (74–420 μm) and fine (44–74 μm) particles of insoluble bone matrix as carriers of BMP-induced bone formation.[27]

Our interpretation of the results in the present study is as follows: the geometry of the interconnected porous structures in PPHAP and coral-HAP create spaces for vasculature that lead to osteogenesis while the smooth structure and close contact of particles in

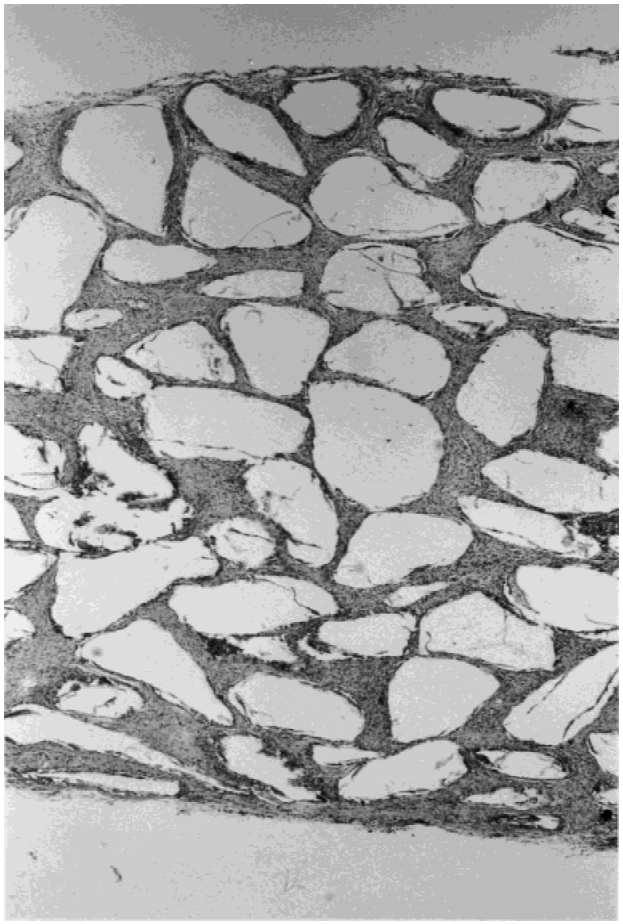

Figure 5. Photomicrograms of the solid particles of hydroxyapatite combined with BMP (SPHAP/BMP) harvested at 3 weeks after implantation. There was no sign of bone or cartilage formation.

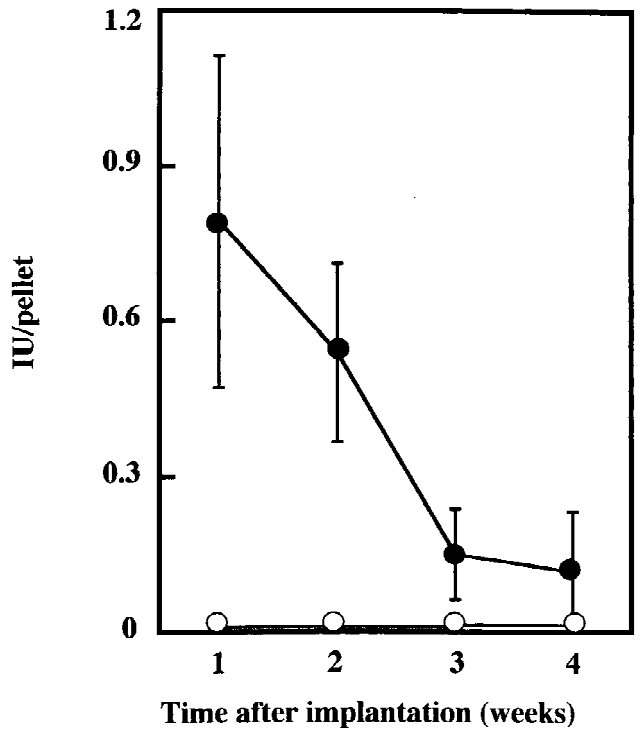

Figure 6. Time-dependent changes of alkaline phosphatase activity in the implants of coral HAP/BMP (indicated by solid circles) and HAP alone (indicated by open circles).

SPHAP inhibit vascular formation and proliferation of mesenchymal cells so that there is no bone or cartilage formation. It is concluded that the geometrical structure of hydroxyapatite ceramics suitable for vasculature leading is crucial for a carrier of BMP-induced bone formation.

What is the feasible geometry of the carrier?

Then what geometry is feasible for vasculature creation? First, there must be interconnected pores of a certain size or space that can lead to vasculature. When we designed the PPHAP in our laboratory, from studies by early workers,[29] we estimated the appropriate optimal pore size to be 150 μm. However, very recently, using a series of block-type porous hydroxyapatite with different pore sizes ranging 106–212, 212–300, 300–400, 400–500, and 500–600 μm, we clearly have shown that the optimal pore size is 300–400 μm. Also, direct bone formation was observed in all the carriers with different sizes, resembling the bone formation in the harvarsian canals.[30]

Also important are the shape, chemical properties, and the inner-surface structures of the pores. At present, we conclude one of the best carriers for BMP-induced osteogenesis to be an interconnected porous hydroxyapatite with a concave, smooth inner surface. Recent Ripamonti et al.[25] reported that coral-HAP functions as a carrier of BMP-induced bone formation when it is used in disk form (7 mm in diameter, 3 mm in height) but not in granular form (400–620 μm in diameter). In this regard, our positive results with the disk-shaped coral-HAP with a diameter of 5 mm and a thickness of 2 mm well agrees with theirs. Our positive results with PPHAP, however, shows a discrepancy with their negative results from coral-HAP of the granular type. It is still unclear why in the study by Ripamonti et al. the particles of coral-HAP (400–620 μm in diameter) did not induce bone effectively while the disk-form of the same coral HAP did well. One possible explanation is that the process of granulation of coral-HAP may damage, at least partially, the interconnections of the pores, which are crucially important for vascularization.

Bone formation on the surface of HAP

Detailed morphological observation of implants of coral-HAP/BMP using double fluorescent labeling of newly formed bone (Fig. 2) revealed that bone formation always started at the surface of the ceramic and then increased in volume, occupying the spaces in and

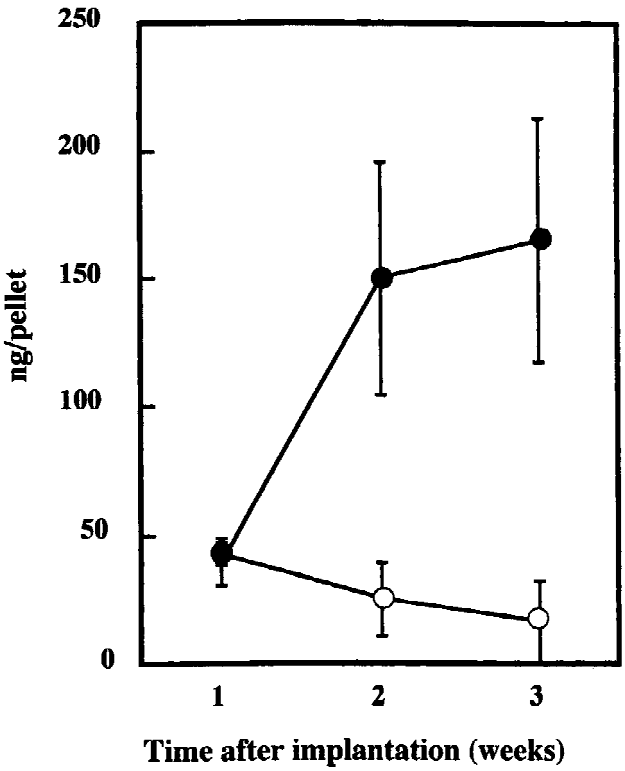

Figure 7. Time-dependent changes of the contents of osteocalcin in the implants of the coralline hydroxyapatite with (–●–) and without (–○–) BMP. Note that only the implant with BMP had increased osteocalcin.

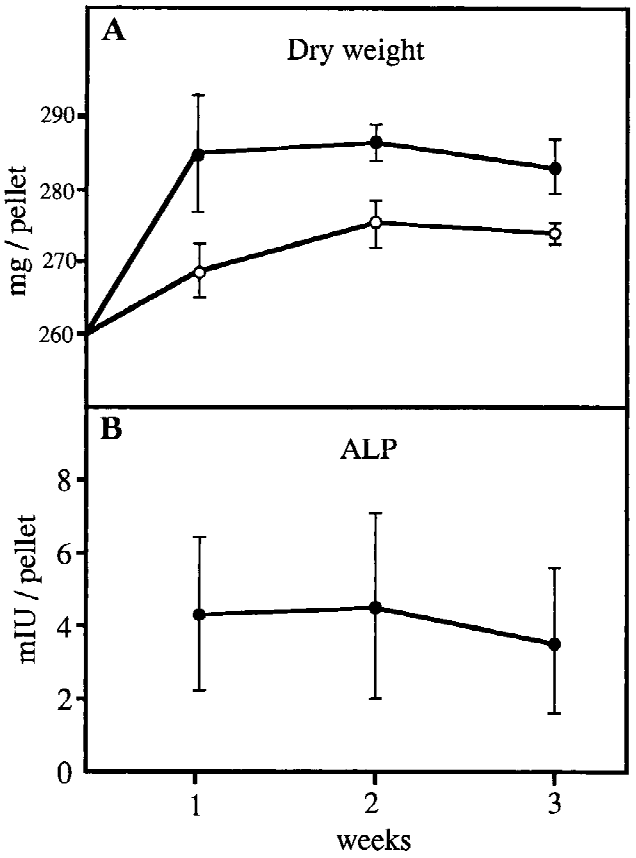

Figure 8. Time-dependent changes of the dry weight (A) and alkaline phosphatase activity (B) of the implants of the solid particles of hydroxyapatite (SPHAP) with (–●–) and without (–○–) BMP. There was no increase in alkaline phosphatase activity although there was a slight increase in dry weight of the SPHAP/BMP implant. Alkaline phosphatase activity of SPHAP without BMP was as low as the level of experimental error.

between the ceramics. Electron probe microanalysis also showed that direct continuity of newly formed bone and ceramics, which is usually formed in the bioactive material/bone interface, was attained. These observations agreed well with our previous report on bone formation on the surface of coral-HAP when the ceramics were implanted with bone marrow cells.[31] In this report, the importance of the interconnected porous geometry in hydroxyapatite ceramics clearly was demonstrated when they were used as the BMP carrier for bone formation. These conclusions will be helpful for further development of technology for local bone reconstruction.

We thank Drs. M. Okumura and K. Inoue (Department of Orthopedics, Nara Medical University) for their contributions in the histological and biochemical analyses of Interpore ceramics. We are also thankful to Drs. H. Itoh and Y. Wakisaka for preparation of the apatite ceramics PPHAP and SPHAP.

References

1. Y. Kuboki, H. Yamaguchi, A. Yokoyama, M. Murata, H. Takita, M. Tazaki, M. Mizuno, T. Hasegawa, S. Iida, K. Shigenobu, R. Fujisawa, M. Kawamura, T. Atuta, A. Matumoto, H. Kato, H.-Y. Zhou, I. Ono, N. Takeshita, and N. Nagai, ''Osteogenesis induced by BMP-coated biomaterials: Biochemical principles of bone reconstruction in dentistry,'' in *The Bone–Biomaterials Interface,* J.E. Davies (ed.), University of Toronto Press, Toronto, 1991, pp. 127–138.
2. M. Mizuno and Y. Kuboki, ''TGF-beta accelerated the osteogenetic differentiation of bone marrow cells induced by collagen matrix,'' *Biochem. Biophys. Res. Commun.,* **211,** 1091–1098 (1995).
3. R. Fujisawa and Y. Kuboki, ''Further characterization of interaction between bone sialoprotein (BSP) and collagen,'' *Calcif. Tissue Int.,* **56,** 140–144 (1995).
4. H. Takita and Y. Kuboki, ''Conformational changes of bovine bone osteonectin induced by interaction with calcium,'' *Calcif. Tissue Int.,* **56,** 559–565 (1995).
5. K. Shigenobu, K. Kaneda, N. Nagai, and Y. Kuboki, ''Localization of bone morphogenetic protein-induced bone and cartilage formation on a new carrier,'' *Ann. Chir. Gynaecol.,* **82,** 85–90 (1993).
6. Y. Sasano, E. Ohtani, K. Narita, A. Kagayama, M. Murata, T. Saito, K. Shigenobu, H. Takita, M. Mizuno, and Y. Kuboki, ''BMPs induce direct bone formation in ectopic sites independent of the endochondral ossification *in vivo,*'' *Anat. Rec.,* **236,** 373–380 (1993).
7. D. Kobayashi, H. Takita, M. Mizuno, Y. Totsuka, and Y. Kuboki, ''Time-dependent expression of bone sialoprotein fragments in osteogenesis induced by bone morphogenetic protein,'' *J. Biochem.,* **119,** 475–481 (1996).
8. M. R. Urist, ''Formation by autoinduction,'' *Science,* **150,** 893–899 (1965).
9. J. M. Wozney, V. Rosen, A. J. Celeste, L. M. Mitsock, M. J. Whitters, R. W. Kriz, R. M. Hiwick, and E. A. Wang, ''Novel regulators of bone formation,'' *Science,* **242,** 1528–1534 (1988).
10. M. Inada, T. Katagiri, S. Akiyama, M. Namiki, M. Komaki, A. Yamaguchi, K. Kamoi, V. Rosen, and T. Suda, ''Bone morphogenetic protein-12 and 13 inhibit terminal differentiation of myoblast, but do not induce their differentiation into osteoblasts,'' *Biochem. Biophys. Res. Commun.,* **222,** 317–322 (1996).
11. Y. Kuboki, T. Saito, M. Murata, H. Takita, M. Mizuno, M. Inoue, N. Nagai, and R. Pool, ''Two distinctive BMP carriers induce zonal chondrogenesis and mambranous ossification, respectively; geometrical factors of matrices for cell-differentiation,'' *Connect. Tiss. Res.,* **32,** 219–226 (1995).
12. T. K. Sampath and A. H. Reddi, ''Dissociative extraction and reconstruction of extracellular matrix components involved in local bone differentiation,'' *Proc. Natl. Acad. Sci. USA,* **78,** 7599–7603 (1981).
13. A. Saito, H. Kato, and Y. Kuboki, ''A study of periodontal regenerative therapy using BMP in horizontal bone defects,'' *Jpn. J. Periodont.,* **36,** 810–822 (1994).
14. Y. Kuboki, M. Sasaki, A Saito, H. Takita, and H. Kato, ''Regeneration of periodontal ligament and cementum by BMP-applied tissue engineering,'' *Eur. J. Oral Sci.,* in press.
15. Y. Kuboki, H. Takita, M. Mizuno, E. Furu-uchi, and K. Taniguchi, ''Separation of bone matrix protein's calcium-induced precipitation,'' *Calcif. Tissue Int.,* **44,** 269–277 (1989).
16. S. Iida, T. Kawasaki, M. Mizuno, and Y. Kuboki, ''Bone formation in osteoporotic rats: Reduced effect of bone morphogenetic protein (BMP) ascribed to the suppressed osteoblast differentiation,'' *Jpn. J. Oral Biol.,* **36,** 249–262 (1994).
17. H. Yamaguchi, ''Purification and characterization of a bone morphogenetic protein derived from bovine bone,'' *Hokkaido J. Dent. Sci.,* **14,** 26–48 (1993).
18. D. M. Roy and S. K. Linnehan, ''Hydroxyapatite formed from

coral skeletal carbonate by hydrothermal exchange,'' *Nature,* **24,** 220–222 (1974).

19. H. Itoh, Y. Wakisaka, Y. Ohnuma, and Y. Kuboki, ''A new porous hydroxyapatite ceramic prepared by cold isostatic pressing and sintering synthesized flaky powder,'' *Dental Mater. J.,* **13,** 25–35 (1993).

20. H. Monma and T. Kamiya, ''Preparation of hydroxyapatite by the hydrolysis of brushite,'' *J. Mater. Sci.,* **22,** 4247–4250 (1987).

21. P. R. N. Kind and E. J. King, ''Estimation of plasma phosphatase by determination of hydrolyzed phenol with amino-antipyrine,'' *J. Clin. Path.,* **7,** 322–326 (1954).

22. H. V. Connerty and A. R. Briggs, ''Determination of serum calcium by means of orthocresolphtalein complexon,'' *Am. J. Clin. Path.,* **45,** 290–296 (1966).

23. J. M. Kissane and E. J. Robins, ''The fluorometric measurement of deoxyribonucleic acid in animal tissues with special reference to the central nervous system,'' *J. Biol. Chem.,* **233,** 184–188 (1958).

24. P. K. Smith, R. I. Krohn, G. T. Hermanson, A. K. Mallia, F. H. Gartner, M. D. Provenzano, E. K. Fujimoto, N. M. Goeke, B. J. Olson, and D. C. Klenk, ''Measurement of protein using bocinchroninic acid,'' *Anal. Biochem.,* **15,** 76–85 (1985).

25. U. Ripamonti, S. MA, and A. H. Reddi, ''The critical role of geometry of porous hydroxyapatite delivery system in induction of bone by osteogenin, a bone morphogenetic protein,'' *Matrix,* **12,** 202–212 (1992).

26. T. K. Sampath and A. H. Reddi, ''Dissociative extraction and reconstitution of extracellular matrix components involved in local bone differentiation,'' *Proc. Natl. Acad. Sci. USA.,* **78,** 7599–7603 (1981).

27. T. K. Sampath and A. H. Reddi, ''Importance of geometry of the extracellular matrix in endochondral bone differentiation,'' *J. Cell Biol.,* **98,** 2192–2197 (1984).

28. A. H. Reddi and C. B. Huggins, ''Influence of transplantation tooth and bone on transformation of fibroblasts,'' *Proc. Soc. Exp. Biol. Med.,* **143,** 634–637 (1973).

29. J. Niwa, M. Munemya, M. Hori, S. Takahashi, M. Ono, and H. Takeuchi, ''Hydroxyapatite as a filling material for bone defect,'' in *Fundamental and Clinical Aspects of Transplantation of Bone and Cartilage,* A. Masumi (ed.), Orthopedics, Nankodo, Tokyo, 1985, pp. 89–95.

30. E. Tsuruga, H. Takita, H. Itoh, Y. Wakisaka, and Y. Kuboki, ''Pore size of porous hydroxyapatite as the cell substratum controls BMP-induced osteogenesis,'' *J. Biochem.,* to appear.

31. H. Ohgushi, Y. Dohi, S. Tamai, and S. Tabata, ''Osteogenic differentiation of marrow stromal stem cells in porous hydroxyapatite ceramics,'' *J. Biomed. Mater. Res.,* **27,** 1401–1407 (1993).